ARTICLE OPEN

Check for updates

# Aberrant ventral dentate gyrus structure and function in trauma susceptible mice

Bart C. J. Dirven[1,2], Dewi van der Geugten[1], Carolina Temporão[1], Miranda van Bodegom[1], Leonie Madder[1], Laura van Agen[1], Judith R. Homberg[1], Tamas Kozicz[2,3,4]✉ and Marloes J.A.G. Henckens[1]✉



Post-traumatic stress disorder (PTSD) is a psychiatric disorder vulnerable individuals can develop following a traumatic event, whereas others are resilient. Enhanced insight into the mechanistic underpinnings contributing to these inter-individual differences in trauma susceptibility is key to improved treatment and prevention. Aberrant function of the hippocampal dentate gyrus (DG) may contribute to its psychopathology, with the dorsal DG potentially encoding trauma memory generalization and the ventral DG anxiety. Using a mouse model, we hypothesized that susceptibility to develop PTSD-like symptoms following trauma will be underpinned by aberrant DG structure and function. Mice were exposed to a traumatic event (unpredictable, inescapable foot shocks) and tested for PTSD-like symptomatology following recovery. In four independent experiments, DG neuronal morphology, synaptic protein gene and protein expression, and neuronal activity during trauma encoding and recall were assessed. Behaviorally, trauma-susceptible animals displayed increased anxiety-like behavior already prior to trauma, increased novelty-induced freezing, but no clear differences in remote trauma memory recall. Comparison of the ventral DG of trauma susceptible *vs* resilient mice revealed lower spine density, reduced expression of the postsynaptic protein *homer1b/c* gene and protein, a larger population of neurons active during trauma encoding, and a greater presence of somatostatin neurons. In contrast, the dorsal DG of trauma-susceptible animals did not differ in terms of spine density or gene expression but displayed more active neurons during trauma encoding and a lower amount of somatostatin neurons. Collectively, we here report on specific structural and functional changes in the ventral DG in trauma susceptible male mice.

*Translational Psychiatry* (2022)12:502 ; https://doi.org/10.1038/s41398-022-02264-7

## INTRODUCTION

Post-traumatic stress disorder (PTSD) is a debilitating disorder one can develop after exposure to a traumatic event. PTSD patients experience excessive arousal, hypervigilance, exaggerated startle responses, and insomnia (DSM-V [1]), which severely impact their quality of life. Moreover, one of the hallmark features of PTSD is the re-experiencing of the trauma through flashbacks, spontaneous recollections, and recurrent nightmares of the trauma [2]. However, whereas over 80% of individuals ever experience a traumatic event, only a relatively small fraction (~15%) will develop PTSD [3, 4]. Understanding the neural basis of this inter-individual variability in PTSD susceptibility is critical for understanding PTSD psychopathology [5], and likely holds unique insights for optimized treatment and even prevention.

An over-generalization of fear to safe, non-trauma-related situations is thought to contribute to PTSD psychopathology [6, 7], but the exact underlying mechanisms remain elusive. Previous research has implicated the aberrant function of the hippocampal dentate gyrus (DG) in fear generalization, impairing hippocampal pattern separation [8], a process resolving interference in encoding and retrieving similar experiences [9–14]. Robust lateral inhibition of DG granule cells by inhibitory interneurons in the hilar region [11, 15] ensures the sparse activation necessary for efficient pattern separation, with a prominent role for somatostatin-expressing (SOM) interneurons [16]. However, pattern separation capacity has mainly been attributed to the dorsal DG (dDG), whereas the ventral DG (vDG) seems to be more involved in affective processing [17–20]. Activity in the vDG is associated with anxiety [18, 21–23], the return of extinguished fear [24], and mediating the anxiolytic effects of antidepressant treatment [25–27]. These findings suggest that the dDG might contribute to PTSD symptomatology by impaired pattern separation processes, whereas the vDG might be implicated by mediating increased anxiety. Supporting a role for aberrant overall DG function in PTSD, patients show poor performance on a memory task testing pattern separation [28], as well as a smaller DG volume [29, 30], which correlates with PTSD symptom severity [29]. Rodent work has added to these findings by showing reduced dendritic complexity and spine density in the DG of animals most sensitive to a trauma [31–34], and a reduced expression of DG synaptic proteins [35]. Importantly, most of these studies did not investigate the DG

[1]Department of Cognitive Neuroscience, Donders Institute for Brain, Cognition and Behaviour, Radboud University Medical Center, 6500 HB Nijmegen, The Netherlands. [2]Department of Medical Imaging, Anatomy, Donders Institute for Brain, Cognition and Behaviour, Radboud University Medical Center, 6500 HB Nijmegen, The Netherlands. [3]Center for Individualized Medicine, Department of Clinical Genomics, and Biochemical Genetics Laboratory, Mayo Clinic, Rochester MN 55905 MN, USA. [4]University of Pecs Medical School, Department of Anatomy, Pecs, Hungary. ✉email: Kozicz.Tamas@mayo.edu; Marloes.Henckens@radboudumc.nl

Received: 28 April 2020 Revised: 18 November 2022 Accepted: 23 November 2022
Published online: 06 December 2022

function and structure along its dorso-ventral axis, and the exact functional and structural changes in the susceptible brain are still largely unknown.

Here, we set out to investigate potential DG abnormalities in a PTSD model in male mice, in which mice were first exposed to a traumatic event (foot shocks) and then behaviorally tested for PTSD-like symptomatology, dissociating susceptible from resilient mice. We compared dorsal and ventral DG structure (neuronal morphology and synaptic protein gene expression) and function (activity during trauma memory encoding and remote recall) between susceptible and resilient mice. Affected genes were followed up by the assessment of synaptic protein levels. Moreover, behavioral readouts of anxiety and fear generalization were assessed prior to or immediately following trauma exposure, to obtain insights into important predictors of later trauma susceptibility.

## MATERIALS AND METHODS

### Animals

The study consisted of four separate experiments: experiment 1 ($n = 24$) to assess DG spine density, experiment 2 ($n = 48$) for assessing DG gene expression, experiment 3 to validate DG gene expression findings at the protein level ($n = 44$), and experiment 4 ($n = 45$) to assess DG neuronal activity. Sample sizes were based on previous experiments with this PTSD model[39,40]. For experiments 1–2, C57BL/6 J mice (Charles River, France) were used. For experiment 3, ArcCreER$^{T2}$xROSA offspring (ArcTRAP [36]) was used that was generated by crossing heterozygote male ArcCreER$^{T2}$ (B6.129(Cg)-*Arc*$^{tm1.1(cre/ERT2)Luo}$/J, 021881, Jackson Laboratory) and homozygote conditional ROSA mice (B6.Cg-*Gt(ROSA)26Sor*$^{tm9(CAG-tdTomato)Hze}$/J, 007909, Jackson Laboratory). For experiment 4, heterozygote male FosCreER$^{T2}$ mice (B6.129(Cg)-*Fos*$^{tm1.1(cre/ERT2)Luo}$/J, 021882, Jackson Laboratory) were crossed with homozygote ROSA females to generate heterozygote offspring (FosTRAP [36]). Based on sex differences in stress sensitivity [37, 38], and the fact that the used PTSD model has only been validated in males [39, 40], only male mice were used. Mice were group housed (3–4 mice per cage) in individually ventilated cages on a reverse 12 hour (9.00–21.00 h) dark/light cycle. Food and water were provided ad libitum. All behavioral testing was performed at least 4 h into the animals' active phase (i.e., the dark). The experimental protocols were in line with international guidelines, the Care and Use of Mammals in neuroscience and Behavioural Research (National Research Council 2003), the principles of laboratory animal care, as well as the Dutch law concerning animal welfare and approved by the Central Committee for Animal Experiments, Den Haag, The Netherlands.

### PTSD model

All mice were exposed to PTSD-induction model (Fig. S1) as described before [39, 40]. On day 1, mice were exposed to a traumatic event, i.e., the exposure to 14 × 1 s 1 mA foot shocks at variable intervals for an 85 min session in a certain context A. Locomotor activity during trauma exposure was assessed by analyzing beam break data, on infrared beams located at both sides of the context. On day 2, 21 h post-trauma, mice were subjected to a subsequent trigger, i.e., 5 × 1 s 0.7 mA foot shocks at a fixed 1-min interval for 5 min session, in a different context (context B). Mice were videotaped during trigger exposure, and videos analyzed for freezing behavior by a researcher blind to the experimental group, to assess novelty-induced anxiety as well as shock-induced fear. Mice were allowed to recover, and at a week post-trauma tested for their behavioral response by assessing PTSD-like behavior; impaired risk assessment (dark-light transfer test), increased anxiety (marble burying), hypervigilance (acoustic startle), impaired sensorimotor gaiting (pre-pulse inhibition), and disturbed circadian rhythm (locomotor activity during the light phase) [40]. Additionally, to assess the neuroendocrine stress response, mice were exposed to restraint stress. See the Supplementary Materials for further details.

### Behavioral categorization

In order to categorize mice as either PTSD-like or resilient, mouse behavior on each of the tests was sorted and the 25% of mice who had the lowest values were attributed 3 points for percentage risk assessment, 3 points for latency to peak startle amplitude, and 2 points for percentage PPI. Similarly, 25% of mice showing the highest values were attributed 1 point for light locomotor activity and marble burying [39]. Points for each test were determined by factor analysis as described before [40]. The points per animal were tallied to generate an overall PTSD symptom score (Fig. S2), and mice that had totals of 5 or more points (necessitating extreme behavior in multiple tests) were termed susceptible. Only mice that had 0 points were termed resilient.

### Experiment 1: DG neuronal morphology

*Sacrifice*. Mice were subjected to the PTSD model and sacrificed under baseline conditions on day 23 under anesthesia (5% isoflurane inhalation followed by i.p. injection with 200 µl pentobarbital) by perfusion with phosphate-buffered saline (PBS) followed by phosphate-buffered 4% paraformaldehyde (PFA). The brains were surgically removed and post-fixed for 24 h in 4% PFA, after which they were transferred to 0.1 M PBS with 0.01% sodium azide and stored at 4 °C.

*Golgi staining*. Brains of susceptible ($n = 4$) and resilient ($n = 5$) mice were processed for rapid Golgi-Cox staining (FD Rapid GolgiStain™ FDNeurotechnologies, Inc. Ellicott City, MD, USA) to examine the neuronal morphology of dorsal and ventral DG granule cells. For every animal, 5 cells per region were reconstructed, on which spines were counted in an average of 6 segments. Statistics were performed on animal averages. Details about the Golgi procedure, neuronal reconstruction, and spine density analysis are given in the Supplementary Materials.

### Experiment 2: DG gene expression

*Design and sacrifice*. Mice in this experiment were first tested in the Open Field and Elevated Plus Maze tests for assessing pre-trauma anxiety (Supplementary Materials). Additionally, the mice were exposed to two functional neuroimaging sessions (7 days prior to trauma induction and 20 days post-trauma) in an 11.7 T BioSpec Avance III small animal MR system (Bruker BioSpin), while anesthetized by 0.5% inhalation isoflurane and subcutaneous infusion of medetomidine (Dexdomitor, Pfizer, 0.1 mg/kg/h [41]). These data are, however, beyond the scope of the present study. Mice were sacrificed on day 28 by rapid decapitation, and brains were surgically removed, quickly frozen on dry ice, and stored at −80 °C until further processing.

*Isolation of target tissue*. Brains of susceptible ($n = 9$) and resilient ($n = 12$) mice from experiment two were sliced into 300 µm coronal slices on a Leica CM3050 S Research Cryostat (Leica Biosystems, Amsterdam, the Netherlands), with a chamber temperature of −12 °C and an object temperature of −10 °C, after which regions of interest were punched out. dDG punches were taken bilaterally with a 0.5 mm diameter hollow needle from three subsequent slices (Bregma −1.70: −2.30 mm), for a total of six punches per subregion. Similarly, six 0.75 mm diameter punches were taken from the vDG (Bregma −2.80: −3.40 mm).

*RNA extraction and cDNA synthesis*. RNA was extracted from the isolated tissue using the AllPrep DNA/RNA Mini Kit (QIAGEN, Venlo, the Netherlands), after which cDNA was synthesized using the SensiFAST™ cDNA Synthesis Kit (Bioline, Taunton, MA, USA).

*Quantitative PCR*. Gene expression was compared in dorsal and ventral DG of susceptible and resilient mice using qPCR. We chose to look specifically at pre- and postsynaptic markers to tie into the spine density measurements and added a spine-localized immediate early gene and a neuronal marker to be able to relate gene expression to the amount of neuronal material included in the punch. Assays included genes encoding synapsin I (*Syn1*) and synaptophysin (*Syp*), both present in synaptic vesicles [42]; postsynaptic density-95 (*Psd-95*), encoding a postsynaptic membrane protein [43]; homer1b/c (*Homer1* splice variant), an postsynaptic density scaffolding protein involved in glutamate receptor transporter protein availability; homer1a (*Homer1* splice variant), an immediate early gene and shown to be in direct competition with the longer transcript homer1b/c [44]; and neurofilament H (*Nefh*), a neuronal marker [35]. Hypoxanthine-guanine phosphoribosyl transferase (*Hprt*) and cytochrome c1 (*Cyc1*) were chosen as housekeeping genes. Details are given in the Supplementary Materials.

### Experiment 3: DG postsynaptic protein expression

*Design and sacrifice*. Mice in this experiment were injected with tamoxifen solution 7 h prior to trauma exposure to label trauma-related

neuronal activity by the induction of tdTomato expression. Since results revealed high background staining in the DG (see Fig. S9), tdTomato signals of this experimental group were not analyzed. On day 23, mice were sacrificed under anesthesia (5% isoflurane inhalation followed by i.p. injection with 200 µl pentobarbital) by perfusion with PBS followed by 4% PFA. Their brains were surgically removed, post-fixed for 24 h in 4% PFA, and stored at 4 °C in 0.1 M PBS with 0.01% sodium azide.

*Immunohistochemistry*. Right hemispheres of the brains of the susceptible ($n = 9$), resilient ($n = 12$) animals were sliced into 30 µm coronal sections and immunostained for Homer1b/c and DAPI. Further details on this cohort are given in the Supplementary Materials.

### Experiment 4: DG neuronal activity

*Design and sacrifice*. Mice in this experiment were injected with tamoxifen solution 7 h prior to trauma exposure to label trauma-related neuronal activity by the induction of tdTomato expression (see Supplementary Materials). On day 23, the FosTRAP mice were placed back in context B for the duration of 10 min, following the exact same procedures as during the trigger session, to induce fear memory recall. No shocks were administered during this context re-exposure session. Behavior was videotaped and freezing behavior was scored manually by an observer blind to the experimental condition (The Observer XT12, Noldus). To confirm successful fear recall in traumatized mice, freezing behavior was compared to that of control mice, which were exposed to the shock boxes without receiving foot shocks. Mice were sacrificed 90 min post re-exposure under anesthesia (5% isoflurane inhalation followed by i.p. injection with 200 µl pentobarbital) by perfusion with PBS followed by 4% PFA. The brains were surgically removed and treated similarly to experiment 3.

*Immunohistochemistry*. Right hemispheres of the brains of the susceptible ($n = 9$), resilient ($n = 8$), and intermediate ($n = 17$) animals were sliced into 30 µm coronal sections and immunostained for c-Fos and somatostatin protein. Further details are given in the Supplementary Materials.

### Statistical analyses

Data were analyzed using IBM SPSS Statistics 23. Data points deviating more than three interquartile ranges from the group median were considered outliers and removed from further analysis (see Supplementary Materials for the exact data points excluded). Normality was checked using the Kolmogorov–Smirnov test. Comparisons between susceptible and resilient animals were done using independent sample *t* tests when assumption for normal distribution was met. In case the assumption for normal distribution was not met, a Mann–Whitney *U* test was used to compare susceptible vs resilient mice. In case of repeated measures within an animal (i.e., effects of dorsal-ventral axis or distance to soma in case of morphological data) a repeated measures ANOVA was used. In case Mauchly's test for sphericity indicated that sphericity could not be assumed, Greenhouse-Geisser tests were reported. Results were considered significant if $p < 0.05$. Significant ANOVA group × axis interaction effects were followed up with *post hoc* independent samples t-tests. Figures show average ± standard of the mean (SEM) in case of normally distributed data, and median ± interquartile distances in case of non-normal distribution.

## RESULTS

### Ventral DG spine density is reduced in male mice susceptible to trauma

To assess potential differences in DG neuronal morphology associated with differential susceptibility to PTSD-like symptoms following trauma, a batch of 24 mice was exposed to the PTSD-induction protocol and, following a week of recovery, assessed on PTSD-like symptomatology (Fig. S3). Susceptible mice were characterized by a significantly higher PTSD-like symptom score than resilient ones ($U = 20$, $p = 0.016$), as well as a suppressed corticosterone stress response (Fig. S4A). DG neuronal morphology of susceptible ($n = 4$) and resilient animals ($n = 5$) was assessed by Golgi staining (Fig. 1A). Sholl analyses revealed no significant differences between groups in the total dendritic material (length) in the dorsal and ventral DG (dDG: $F(1,7) = 1.041$, $p = 0.342$, vDG: $F(1,7)<1$), nor in its distribution across distance to soma (group × distance interaction. dDG: $F(24,168) = 1.010$, $p = 0.456$, vDG: $F(22,154) = 1.037$, $p = 0.424$), whereas there was a clear effect of distance to soma (dDG: $F(24,168) = 62.784$, $p < 0.001$, vDG: $F(22,154) = 50.742$, $p < 0.001$, Fig. 1B). Spine density was comparable between susceptible and resilient mice in the dDG ($U = 10$, $p = 1.000$), but susceptible animals displayed a slightly, but significantly, reduced spine density in the vDG ($U = 0$, $p = 0.029$, Fig. 1C). No significant group differences were observed in either the dendritic trunk length (dDG: $t(7) = 0.085$, $p = 0.935$, vDG: $U(9) = 5$, $p = 0.286$, Fig. S5A) or position within the granule cell layer (dDG: $U(9) = 7$, $p = 0.556$, vDG: $t(7) = -0.569$, $p = 0.587$, Fig. S5B) of the neurons traced. Both these measures are potential indicators of the developmental stage at which the traced neurons were born [45], suggesting that differences between susceptible and resilient mice were not caused by a selection bias towards either older or younger neurons. Yet, as information on trunk length, as well as the location of the soma within the granule cell layer, do not allow for the distinction between mature and immature neurons, it remains to be determined whether phenotypic differences are observed for both types of granule cells or primarily affect one over the other.

### *Homer1b/c* expression is reduced in the ventral DG of mice susceptible to trauma

Next, potential differences in DG gene expression associated with differential susceptibility to PTSD-like symptoms following trauma were assessed in a new batch of 48 mice. To test whether pre-trauma anxiety constitutes a risk factor for later PTSD development, all animals of this batch were additionally tested for anxiety-like behavior prior to trauma exposure.

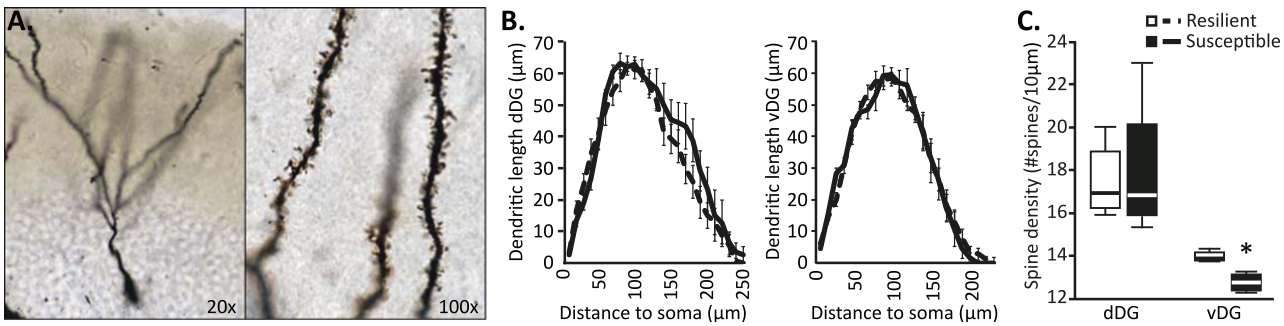


**Fig. 1 Morphology of DG granule cells in susceptible and resilient mice.** Reconstruction of Golgi-stained DG granule cells (**A**) in behavioral cohort 1 revealed no differences in dendritic length between the dorsal (dDG) or ventral DG (vDG) (**B**), but indicated reduced spine density in the ventral DG of susceptible animals, whereas no differential spine density was observed in the dorsal DG (**C**). Behavioral results for this cohort are depicted in Figure S3. *$p < 0.05$.

Animals later categorized as susceptible ($n = 10$) *vs* resilient ($n = 12$) (Fig. S6) significantly differed in their PTSD-like symptom score ($U = 108$, $p < 0.001$), but not in their corticosterone stress response (Fig. S4B). Moreover, they did not display different behavior in the open field test prior to trauma exposure. The distance traveled through the center, total distance traveled, the number of crossings through the center, the time spent in the center (all t(20)'s < 1) and the latency to enter the center ($t(20) = 1.581$, $p = 0.129$) of the open field (t(20) < 1) were not different between groups (Fig. S7A). However, groups did differ in the distance traveled on the open arms of the elevated plus maze ($t(19) = 2.307$, $p = 0.033$), with the susceptible animals walking a shorter distance (mean ± stdev: 137.56 ± 51.02 cm) compared to the resilient animals (197.99 ± 64.84 cm). No differences were observed in the time spent on the open arms ($t(20) = 1.395$, $p = 0.178$), nor in the total distance traveled on the maze ($t(11.812) = 1.005$, $p = 0.335$, Fig. S7B). Interestingly, significant behavioral differences between susceptible vs resilient groups were also observed during the trigger session, where the susceptible mice showed a shorter latency to start freezing than resilient animals ($U = 22$, $p = 0.017$). Furthermore, a majority of susceptible mice –in contrast to resilient mice– showed freezing behavior before the first foot shock was administered in this novel context ($U = 88$, $p = 0.020$, Fig. 2A). Subsequent shock-induced freezing was not different between susceptible and resilient ones ($t(20) = 1.216$, $p = 0.238$, Fig. 2A), suggesting similar threat coping mechanisms.

We continued with analyzing the DG's expression levels of genes encoding excitatory presynaptic (*Syn* and *Syp*) and postsynaptic (*Homer1b/c* and *Psd-95*) markers related to spine density, a spine-localized immediate early gene (*Homer1a*) and a neuronal marker (*Nefh*), previously found to be affected by stress [35, 46]. The dorsal (Fig. 2B) and ventral DG (Fig. 2C) did not reveal differential expression of *Nefh* mRNA between susceptible vs resilient mice ($p$'s > 0.13), suggesting that the number of neurons did not differ between groups [35]. Moreover, no differences were found in mRNA levels of the presynaptic vesicle markers *Syn* and *Syp* ($p$'s > 0.1), indicating that synaptic release in the susceptible mice was not altered. Interestingly, mRNA levels for *Homer1b/c* showed a main effect of axis ($F(1,13.058) = 41.810$, $p < 0.001$), group ($F(1,14.981) = 4.868$, $p = 0.043$) and a group × axis interaction ($F(1,13.058) = 34.321$, $p < 0.001$), which was caused by substantially lower expression in the vDG of susceptible animals compared to resilient animals ($t(7.388) = 3.475$, $p = 0.009$), but not the dDG ($t(6.285) = 1.107$, $p = 0.309$). These effects seemed to be driven by three susceptible animals that showed extremely low levels of *Homer1b/c* expression (<1% of the levels of resilient animals), but exclusion of these animals still revealed significant group differences ($t(13) = 2.540$, $p = 0.025$). No differences in the *Homer1a* splice variant were observed between groups ($p$'s > 0.35). Moreover, no group differences in *Psd-95* mRNA levels were observed ($p$'s > 0.23).

To test whether these differences in *Homer1b/c* expression translate to the protein level, we assessed Homer1b/c protein levels in the dDG and vDG by immunohistochemistry in a new cohort of 44 mice, dissociating the molecular layers in the upper and lower blade of the DG, as well as the hilar region. Mice were behaviorally phenotyped and susceptible ($n = 12$) and resilient ($n = 10$) mice identified. Susceptible animals showed a significantly higher PTSD-like symptom score ($U(21) = 120$, $p < 0.001$, Fig. S8), as well as trend-level significant reductions in corticosterone stress levels (Fig. S4C). Homer1b/c expression was quantified in each DG subregion by analyzing both total cluster area size (reflecting postsynaptic density (PSD) size [47, 48]), as well as cluster signal intensity (Fig. 2D), as a proxy for protein expression levels [49]. Whereas no differences in cluster area size were observed in any of the dDG and vDG subregions (all $p$'s > 0.167), signal intensity tended to be lower in the molecular layer of the upper blade of the vDG ($t(14) = 1.893$, $p = 0.079$), and this reduction reached significance in the molecular layer of the lower blade of the vDG ($t(14) = 2.375$, $p = 0.032$, Fig. 2E) in susceptible mice. No differences in signal intensity were observed in the ventral hilar region ($U(17) = 36$, $p = 1.00$), nor in any of the dDG subregions (all $p$'s > 0.21), suggesting a specific effect for the vDG molecular layer.

**Trauma susceptible mice exhibit larger DG neuronal ensemble activation during trauma encoding**

Next, we wanted to investigate whether differential trauma susceptibility was also related to distinct DG functionality in terms of its activity during trauma memory encoding and retrieval. To do so, we used FosTRAP mice [36], in which the injection of tamoxifen induces the expression of the fluorescent marker tdTomato in all c-Fos-expressing (i.e., activated) neurons. For the study of DG function, the FosTRAP mouse line was preferred over the ArcTRAP mouse line [36, 50, 51], as the latter is characterized by substantial background staining of DG neurons in non-injected animals (i.e., labeled neurons in the absence of tamoxifen (Fig. S9)), which is not observed in FosTRAP mice (Fig. S10) [36]. Pilot experiments indicated that FosTRAP mice showed no alterations in fear behavior or memory performance, and significant labeling of DG neuronal activity upon tamoxifen injection (Fig. S10, S11), qualifying them for the experiment.

To investigate whether DG activity during trauma encoding can predict trauma susceptibility, we injected 40 FosTRAP mice with tamoxifen prior to trauma induction, followed by the trigger the next day. Again, following a week of recovery, mice were tested for PTSD-like symptoms, dissociating susceptible ($n = 9$) from resilient ($n = 8$) mice (Fig. S11) with differing PTSD-like symptom scores ($U = 72$, $p < 0.001$). Susceptible mice also showed a suppressed corticosterone stress response (Fig. S4D). To additionally test whether trauma susceptibility is associated with altered DG recruitment during the recall of the traumatic experience, animals were re-exposed to the trigger context prior to sacrifice, and their brains analyzed for recall-induced c-Fos expression. To compare behavioral responses as well as neuronal activity during trauma exposure and remote memory recall to that of a neutral memory, we also included control animals ($n = 5$, randomly assigned). Control animals were injected with tamoxifen at the same time point as the trauma group, but did not receive any foot shocks, nor were they tested for PTSD-like symptomatology to prevent testing-induced stress.

As expected, during the trigger session controls started freezing later than both shock-exposed groups (median ± interquartile range: 68.68 ± 106.82, $U = 10$, $p < 0.001$), and froze less following shock delivery in the shock-exposed group (mean ± stdev: 0.84 ± 0.57 s, $t(35.917) = 27.713$, $p < 0.001$).

Moreover, control mice displayed lower freezer behavior during the first minute of the trigger session (i.e., prior to the first shock administration in the shock-exposed groups) (mean ± stdev: 13.14 ± 11.13 s, $t((15.759) = 6.086$, $p < 0.001$), suggesting increased context-induced anxiety in shock-exposed mice. Retrospective analyses revealed no differential locomotor behavior in the trauma context between susceptible *vs* resilient mice (overall mobility; t(12) < 1). However, significant differences were again observed between groups during the trigger session, when the susceptible mice showed a shorter latency to start a freezing bout (defined as a period of complete immobility for >2 s) than resilient animals ($t(8.910) = 2.374$, $p = 0.042$), and on average started freezing well before the first foot shock administration in this novel context (Fig. 3A). Overall freezing prior to the first shock administration was not different between susceptible and resilient animals (t(13) < 1), nor were subsequent shock-induced freezing levels ($t(12.786) < 1$, $p = 0.561$, Fig. 3A).

During the re-exposure to the trigger context to induce memory recall, control animals again displayed a longer latency to start freezing than shock-exposed animals (median ± interquartile

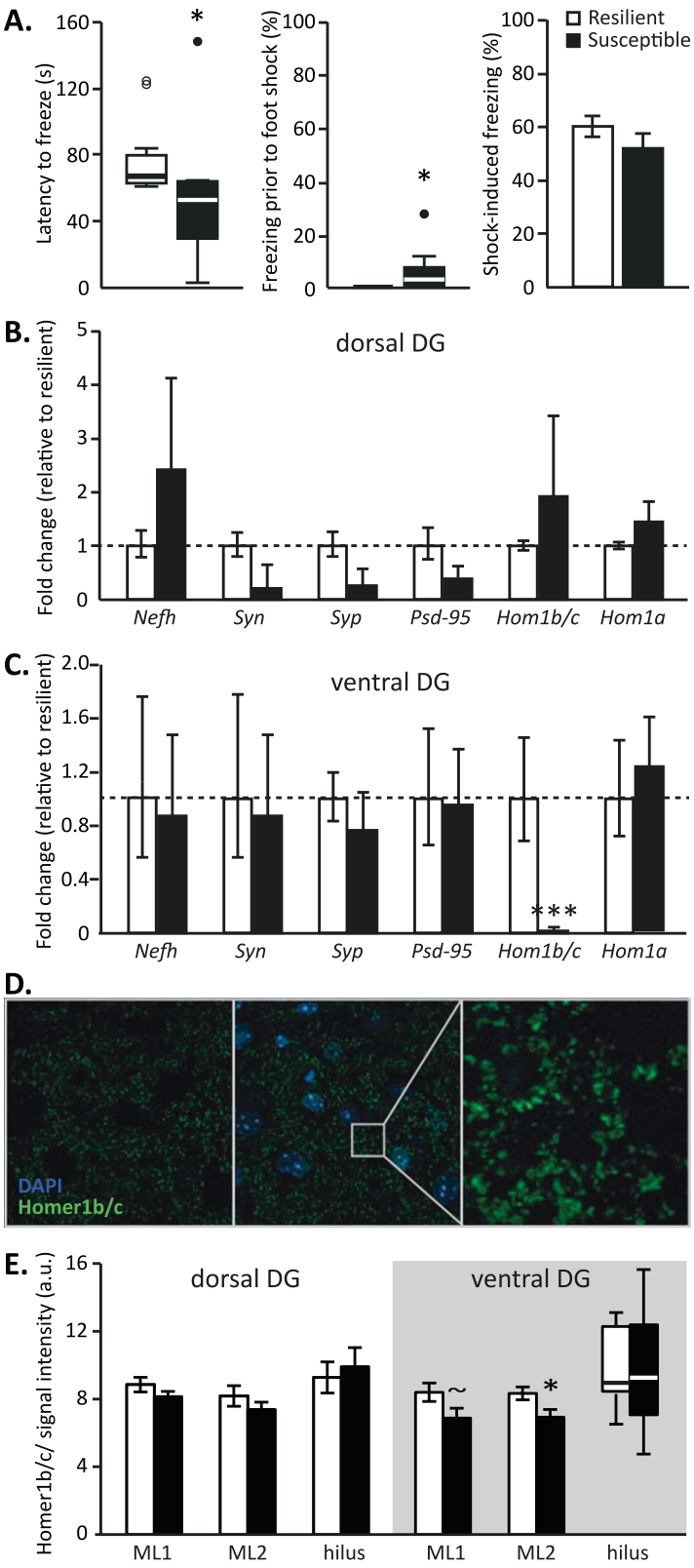


range: 235.18 ± 361.37 s, $U = 6$, $p < 0.001$) and overall froze less (mean ± stdev: 0.58 ± 0.53 s, $F(1,40) = 8.157$, $p = 0.007$), supporting the existence of a fear memory in the mice subjected to the PTSD-induction protocol compared to the controls. In contrast to the shorter latency to start freezing observed during the trigger exposure, susceptible animals tended to show a somewhat longer latency to start freezing during its recall ($t(8.314) = 2.119$, $p = 0.066$, Fig. 3B). Examination of the freezing levels of susceptible and resilient animals over time revealed a significant effect of time ($F(3.897,54.561) = 3.081$, $p = 0.024$), with freezing

**Fig. 2 Behavioral freezing (cohort 2) and synaptic protein (gene) expression in the DG of susceptible and resilient mice.** Susceptible animals showed a lower latency to freeze in the trigger context, with substantial freezing already prior to the first foot shock in this novel context. Subsequent shock-induced freezing was not different between groups (**A**). Gene expression levels of synaptic proteins were not different between susceptible and resilient animals in the dorsal dentate gyrus (DG) (**B**), but revealed a strong reduction in the expression of the Homer1b/c gene (*Hom1b/c*) in the ventral DG (**C**). Behavioral results for cohort 2 on PTSD-like symptoms are depicted in Figure S6, whereas anxiety measures are displayed in Figure S7. Behavioral cohort 3 was used for immunohistochemistry experiments aimed at validating that *Hom1b/c* gene expression differences translated to the protein level. Homer1b/c protein expression levels were assessed in the upper (ML1) and lower (ML2) molecular layers, as well as the hilus of the dorsal and ventral DG (**D**, **E**). Susceptible animals appeared to be characterized by lower Homer1b/c expression in the ventral DG molecular layers, but not ventral hilus or dorsal DG (**E**). Behavioral results for cohort 3 on PTSD-like symptoms are depicted in Figure S8. *Nefh*: neurofilament H, *Syn*: synapsin I, *Syp*: synaptophysin, *Psd-95*: postsynaptic density-95, *Hom1a*: Homer1a splice variant, $^{\sim}p = 0.079$, $^{*}p < 0.05$, $^{***}p < 0.001$.

reducing upon prolonged context exposure, but no differences between groups (main effect of group; $F(1,14) = 1.279$, $p = 0.277$, group × time interaction; $F(3.897,54.561)<1$, Fig. 3B).

Neurally, shock-exposed animals did not show different active neuronal populations in the DG during the trauma and trigger exposure compared to controls (main effect of trauma exposure; $F(1,34) = 1.459$, $p = 0.235$, trauma exposure × axis interaction; $F(1,34) < 1$)), whereas overall a higher density of active neurons was found in the dorsal DG ($F(1,34) = 13.781$, $p < 0.001$) (mean ± stdev: $dDG_{trauma} = 19.06 \pm 8.70$, $dDG_{control} = 25.16 \pm 7.55$, $vDG_{trauma} = 15.64 \pm 7.60$, $vDG_{control} = 18.56 \pm 6.22$). DG activity during fear memory recall as assessed by c-Fos expression was also not significantly different between groups (main effect of trauma exposure; $F(1,31) < 1$, trauma exposure × axis interaction; $F(1,31) = 1.070$, $p = 0.309$), but again higher in the dorsal than ventral DG ($F(1,31) = 6.898$, $p = 0.013$) ($dDG_{trauma} = 28.27 \pm 12.5$, $dDG_{control} = 33.80 \pm 16.08$, $vDG_{trauma} = 23.90 \pm 12.48$, $vDG_{control} = 23.08 \pm 5.89$). Control animals showed significantly higher reactivation rates in the dorsal DG during trauma recall (median ± interquartile range: $dDG_{trauma} = 0.71 \pm 1.31\%$, $dDG_{control} = 1.28 \pm 1.81\%$, $U = 31$, $p = 0.025$), potentially reflecting increased similarity between encoding and recall conditions in this group. No differences were observed in reactivation rates in the ventral DG (median ± interquartile range: $vDG_{trauma} = 0.00 \pm 0.53\%$, $vDG_{control} = 0.39 \pm 1.35\%$, $U = 50$, $p = 0.200$). The number of somatostatin neurons was not different between groups, nor was their activity during 'trauma' encoding and recall (all $p$'s > 0.05).

When comparing the DG neuronal populations active during the trauma and trigger exposure (i.e., the number of tdTomato-expressing neurons) in susceptible *vs* resilient mice revealed that the susceptible animals displayed a significantly larger active neuronal ensemble during the PTSD-induction protocol compared to resilient animals (main effect of group; $F(1,12) = 4.841$, $p = 0.048$), and that this difference was independent of ventral-dorsal axis (group × axis interaction; $F(1,12) < 1$, Fig. 4B). The amount of active DG neurons during fear memory recall as assessed by c-Fos expression was not significantly different between groups (main effect of group; $F(1,12) < 1$, group × axis interaction; $F(1,12)<1$, Fig. 4C). In terms of the reactivation rates (defined as the number of neurons double-positive for tdTomato and c-Fos divided by the total number of tdTomato positive cells [52, 53]), no significant group differences were observed for the dDG (median ± interquartile range: $dDG_{resilient} = 0.44 \pm 2.20\%$, $dDG_{susceptible} = 0.00 \pm 1.21\%$, $U = 19.5$, $p = 0.573$), whereas the vDG revealed trend-level significant higher reactivation in susceptible *vs* resilient mice (median ± interquartile range: $vDG_{resilient} = 0.00 \pm 0.00\%$, $vDG_{susceptible} = 0.41 \pm 1.88$, $U = 32.5$, $p = 0.065$). However, reactivation rates were overall very low. Remarkably, the number of DG somatostatin neurons –primarily located in the DG hilar region (Fig. 4A)– was significantly lower in the dDG of susceptible *vs* resilient mice ($t(12) = 2.691$, $p = 0.020$), whereas a trend towards increased counts of somatostatin neurons was observed in the vDG ($t(11) = 1.845$, $p = 0.087$), resulting in a significant group × axis interaction ($F(1,10) = 8.511$, $p = 0.015$, Fig. 4D). Both the number of active DG somatostatin neurons during encoding and remote recall were very low (Table S1) and not different between groups (all p's > 0.5).

Based on significant correlations between overall PTSD-like symptom score and the number of active neurons in the vDG during the trauma and trigger exposure (i.e., number of tdTomato positive cells; $\rho(14) = 0.703$, $p = 0.005$), as well as the number of somatostatin neurons within the vDG ($\rho(13) = 0.623$, $p = 0.023$), we additionally analyzed the brains of 17 animals that showed an intermediate PTSD phenotype ($1 \leq$ PTSD-like symptom score $\leq 4$). All DG outcome measures were subsequently tested for significant associations with PTSD-like symptom score, instead of group differences between the extreme-scoring animals only. These analyses confirmed previous findings of a larger active DG population during trauma+trigger processing predicting greater PTSD-like symptomatology ($\rho(30) = 0.426$, $p = 0.019$), and suggested that this correlation was particularly prominent for the vDG ($\rho(30) = 0.420$, $p = 0.021$, Fig. 4E), whereas the association between PTSD-like symptom score and dDG activity failed to reach significance ($p = 0.153$, Fig. S12A). Furthermore, these analyses confirmed an increased presence of somatostatin neurons in the vDG (but no differences in the dDG; $\rho(29) = -0.028$, $p = 0.884$, Fig. S12B) in the development of PTSD-like symptomatology, although this association reached trend-level significance only ($\rho(29) = 0.354$, $p = 0.059$, Fig. 4G). When testing for correlations between the number of active DG neurons and trauma memory recall, DG activity during trauma encoding appeared not predictive of later re-exposure-induced freezing ($p$'s > 0.5), but increased recall-induced activity in the dDG ($\rho(31) = 0.495$, $p = 0.005$, Fig. 4F) (but not vDG ($p = 0.236$)) was associated with enhanced memory recall. These data implicate particularly the dDG in fear memory recall, which seems unaffected in susceptible compared to resilient animals. Deviations in vDG function however seem to correlate more strongly with differences in PTSD-like symptomatology.

## DISCUSSION

We investigated the association between DG structure and function and the susceptibility to develop PTSD-like symptoms following trauma. Besides trauma-induced PTSD-like symptomatology, susceptible animals displayed increased anxiety-like behavior already prior to trauma, and greater anxiety in a novel context following trauma exposure. No clear differences between susceptible and resilient mice were observed in remote trauma memory recall. Comparison of the vDG of susceptible *vs* resilient mice revealed lower spine density, reduced expression of the postsynaptic protein *homer1b/c* gene and protein, increased population of neurons active during trauma encoding, and increased presence of somatostatin neurons to be associated with trauma susceptibility. In contrast, the dDG of susceptible animals did not differ in terms of spine density or synaptic protein gene expression, but displayed more active neurons during trauma encoding and fewer somatostatin neurons. As such, these data implicate mainly the vDG in establishing PTSD-like symptoms of trauma-related arousal in this animal model.

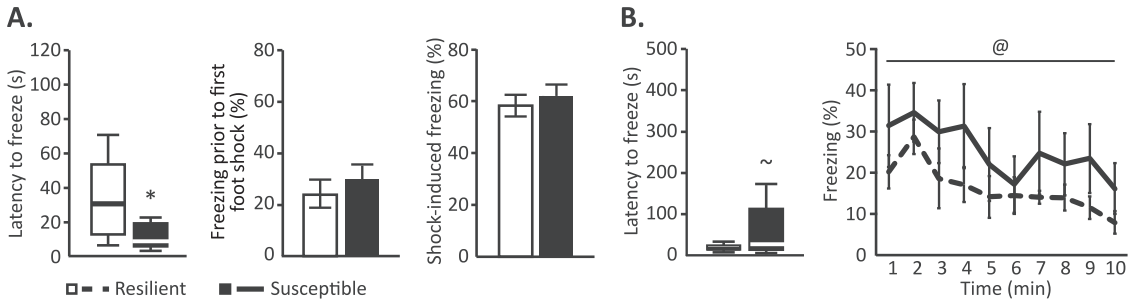


**Fig. 3 Behavioral freezing in susceptible and resilient mice (cohort 4).** Behavioral assessment of cohort 4 confirmed a shorter latency to freeze in susceptible animals in the trigger context (**A**), and revealed a trend towards a longer latency to freeze upon re-exposure to this context compared to resilient animals (**B**), with no differences in overall freezing levels or their reduction across prolonged exposure between these groups. Behavioral results on PTSD-like symptoms for this cohort are depicted in Figure S12. $^{*}p < 0.05$, $^{\sim}p = 0.066$, effect of PTSD-like phenotype; $^{@}p < 0.05$, effect of time.

Here, we used an animal model for PTSD that induces substantial heterogeneity in the behavioral consequences of trauma exposure (i.e., risk assessment, anxiety, hypervigilance, pre-pulse inhibition, and activity during the inactive phase) in male mice. Noteworthy, mice were classified as susceptible or resilient based on a compound score comprising multiple behavioral PTSD-like symptoms, rather than single behavioral features. This classification resembles the situation in patients [54], which can be diagnosed with PTSD based on 20 criteria across four distinct symptom categories, resulting in a highly heterogeneous patient population (DSM-V [1]). Accordingly, we observed substantial behavioral variability both within and across the four different cohorts in this study, as well as when comparing our findings to previous reports on this PTSD model [39, 40]. However, altered vDG function/structure was observed for all cohorts, supporting its involvement in a wide range of PTSD symptoms. Besides modeling behavioral phenotypic traits resembling symptoms in PTSD patients, the animal model recapitulates deviations in the hypothalamic-pituitary-adrenal (HPA) axis response to stress (i.e., suppressed stress peak corticosterone levels [40]), which were previously linked to increased glucocorticoid receptor expression in the ventral subiculum of susceptible animals [40]. In line with this, the HPA axis in PTSD patients seems to be characterized by enhanced negative feedback inhibition (for review, see [55]). However, patient findings are not always consistent (for meta-analyses, see [56, 57]), and it has been suggested that clinically and biologically distinct subtypes of PTSD exist, with only specific subtypes displaying enhanced negative feedback [58, 59]. Likewise, we here did not observe similarly suppressed corticosterone responses across behavioral cohorts. Future studies should investigate if the DG of susceptible mice is characterized by alterations in corticosteroid receptor expression, and how this relates to the aberrancies in HPA axis function.

Dissociating susceptible *vs* resilient animals, we found that susceptible mice traveled shorter distances on the open arms of the elevated plus maze, indicative of a reluctance to explore relative danger zones, reflecting increased anxiety. However, no behavioral differences were observed in the open field, a potentially less adverse environment. These findings match prior animal work on reduced exploratory drive [60] and enhanced anxiety [61] predicting trauma sensitivity, as well as human reports on trait anxiety being predictive of PTSD risk and symptom severity [62, 63]. Furthermore, susceptible animals displayed increased behavioral freezing upon exposure to the unfamiliar trigger context post-trauma. This is in line with reports on elevated distress/arousal soon after trauma being predictive of later PTSD symptom severity [64, 65] and intrusions [66]. It is tempting to relate the increased novelty-induced anxiety to generalized fear in susceptible mice, as has been reported by others [67], but future dedicated assays on the extent to which fear generalizes across contexts are required to warrant such a claim.

Susceptible animals revealed decreased spine density specifically in the vDG, but no differences in dorsal or ventral DG dendritic length. Alterations in DG morphology have been linked to inter-individual differences in stress susceptibility before, with only the animals most susceptible to trauma [32, 34], learned helplessness [33], or chronic social defeat [68] showing reductions in DG spine density. In our PTSD mouse model these effects seem to apply to the vDG specifically. Similarly, we observed a reduction in the expression of the postsynaptic protein *homer1b/c* gene in the vDG, as well as lower Homer1b/c expression levels in the vDG molecular layer. Homer1b/c is an excitatory postsynaptic density scaffolding protein [44], regulating spine morphogenesis, synaptic plasticity and the stabilization of synaptic changes during long-term potentiation (LTP) [48]; suggesting an active role in behavioral plasticity [69]. Its hippocampal expression levels have been found reduced following traumatic stress and are associated with generalized fear [35]. Previous work has also described alterations in the other synaptic genes assessed following stress or trauma [35, 46], but our study is the first in assessing alterations in specifically the DG and contrasting susceptible *vs* resilient individuals, providing more nuance to earlier findings. A limitation is that we measured protein expression levels through immunohistochemistry, instead of Western blots, although this has the benefit of increased spatial specificity. Overall, our assessments of DG synaptic contacts suggest altered vDG synaptic signaling of glutamatergic input, without any dDG differences.

Importantly, larger active populations of DG neurons during trauma encoding predicted later PTSD symptoms, predominantly in the vDG, where the number of active neurons significantly correlated with PTSD-like symptom score. These findings correspond with the suggested role for the vDG in mediating anxiety-related behaviors [18, 21–23], and a reduction of vDG neuronal activity during anxiogenic situations conferring stress resilience [70]. In contrast, larger dDG neuronal populations active during trauma encoding predicted increased freezing upon remote memory recall, which supports its critical role in fear memory acquisition [18, 71, 72]. DG activity is under tight control of local GABAergic interneurons [11, 15, 73], with a prominent role for somatostatin-expressing interneurons [16], which increase the threshold of input required for acquisition of new memories, filtering out irrelevant environmental cues [74]. Correspondingly, activation of somatostatin neurons has been found to reduce the size of the activated granule cell population upon encoding to ensure memory specificity [16]. The reduction in dDG somatostatin neurons and increased number of DG granule cells fit these observations. Similarly, a recent report showed that the activation of a larger DG granule cell ensemble upon fear memory formation results in fear memory generalization [75], matching our findings. No differences between phenotypes were observed in DG activity during memory recall, nor reactivation rates. Although reactivation

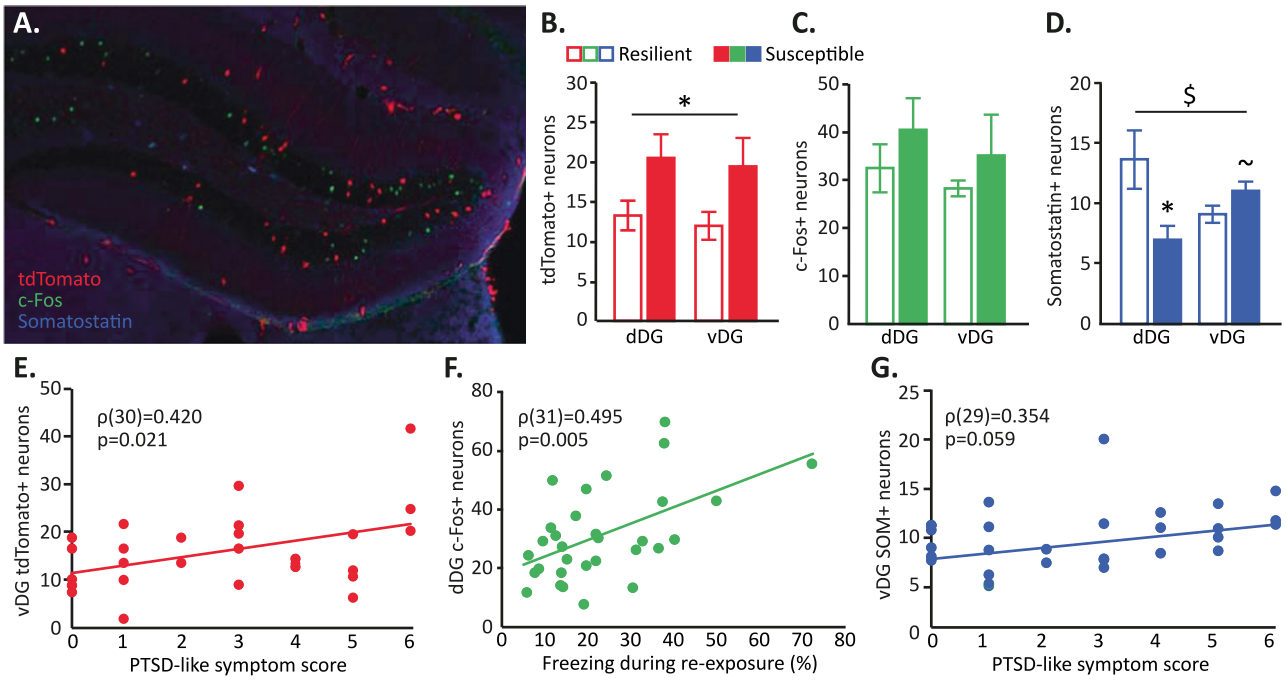


**Fig. 4 DG somatostatin expression and neuronal activity related to trauma encoding and recall in susceptible and resilient mice.** In cohort 4, dentate gyrus (DG) activity during trauma memory encoding (marked by tdTomato expression), remote trauma memory recall (marked by c-Fos expression), as well as somatostatin (SOM) interneuron levels were assessed by immunohistochemistry (**A**). Susceptible animals displayed an increased population of DG neurons active during trauma encoding (**B**), but no differences during its remote retrieval (**C**). The number of somatostatin neurons identified in the dorsal (dDG) and ventral (vDG) differed between groups as well (**D**). Correlational analyses involving also mice with an intermediate PTSD phenotype revealed associations between specifically the ventral DG and PTSD symptom score (**E**, **G**), whereas the dorsal DG seemed to relate to trauma memory strength (**F**). Quality checks for the FosTRAP method are presented in Figures S9 to S11. *$p < 0.05$, ~$p = 0.087$, effect of PTSD phenotype; $^{\$}p < 0.05$, hippocampal axis × PTSD-like phenotype interaction.

of DG neurons activated during encoding has been shown to suffice to induce recent memory recall [76, 77], memories are known to reallocate to either cortical representations over time [78, 79], or to different cells within the hippocampus [80]. This might explain our low DG reactivation rates upon remote recall [50]. Altogether, these findings suggest that aberrant activity of the vDG is implicated in establishing PTSD trauma-related and arousal symptoms modeled in our mouse model, whereas the dDG seems to be more involved in actual trauma memory processing, which seems unaffected here. Noteworthy, the absence of a clear memory recall phenotype, as might be expected in PTSD[1], may suggest that our model strongly relies on the trauma-related arousal and reactivity' symptom cluster of the DSM-V[1]. As such, our PTSD model may have high validity to study excessive post-trauma anxiety, but other models may be better suited to study memory-related abnormalities. However, these abnormalities could also surface only upon re-exposure to a broad array of contexts (testing for fear generalization/pattern separation), or prolonged exposure triggering fear extinction, in which the DG is also involved [81, 82].

Findings of an increased vDG population of active neurons during trauma memory processing may seem at odds with the increased potential for inhibition (i.e., more somatostatin neurons) and reduced capacity for excitation (a reduction in glutamatergic spines and excitatory postsynaptic scaffolding protein gene expression). However, all assessments of DG excitatory/inhibitory structural markers have been obtained post-trauma, posing the question of whether these are cause or consequences of the acquired symptomatology. Previous research has implicated aberrant hippocampal function and structure as both [83, 84]. Therefore, it could well be that the observed alterations in excitatory/inhibitory regulation reflect a compensatory response to an initial excess of excitatory input [85]. However, prior observations that particularly vDG granule cell morphology is related to overall anxiety-like behavior, independent of an animal's stress history [31], may suggest that these alterations are rather caused than a consequence of trauma-associated symptoms. Interestingly, we also observed a significant correlation between vDG *homer1b/c* gene expression and pre-trauma anxiety (distance moved on open arm; $\rho(17) = -0.498$, $p = 0.042$), supporting that the synaptic differences are a pre-disposing trait rather than a state marker of pathology.

Some limitations should be mentioned. Firstly, the structural assessments of glutamatergic/GABAergic regulation cannot directly be related to the neurons involved in trauma memory processing, as these implicate generic DG changes independent of the functional population. Future studies should further investigate this by analyzing morphology and gene expression patterns of trauma-activated neurons specifically. Secondly, we did not consider the heterogeneity of DG granule cells in terms of age. Whereas particularly newborn neurons seem to be involved in pattern separation [86, 87], we most likely mainly included mature granule cells into our analyses, since vast majority of the DG granule cell population is mature [88–90]. Future studies should assess the structure and function of DG newborn neurons in this PTSD model. Thirdly, similar to other hippocampal memory engram labeling studies [76, 91, 92], almost exclusively excitatory cells were labeled by tdTomato expression, leaving the contribution of local interneurons unresolved. Also, the majority of the behavioral cohorts lacked comparison to naïve control mice. Control groups that were subjected to behavioral testing were originally included in these experiments, but the associated stress exposure disqualified them as adequate controls. Inclusion of non-stressed (naïve) control mice instead, would have allowed us to additionally assess the main effects of trauma exposure, and subsequently determine whether differences between susceptible

and resilient phenotypes were related to either excessive (maladaptive) responses or the lack of adaptive responses to stress in susceptible mice. Future studies should include these comparisons. Lastly, current observations are only descriptive and further mechanistic studies will be necessary to elucidate a causal link between the observed vDG alterations and trauma-related behavior.

Concluding, we found little evidence for aberrant dDG structure and function being related to PTSD-like symptomatology in our PTSD model. In contrast, the vDG displayed several deviations indicative of aberrant glutamatergic and GABAergic regulation of granule cell activity in PTSD susceptible mice compared to those that are resilient. These changes appeared associated with elevated anxiety-like behavior even prior to trauma exposure, and higher (generalized) fear to novel contexts. Thereby, the vDG seems critically involved in establishing the PTSD-like symptoms as assessed in our mouse model, and may be an important target for further research into the psychopathology of PTSD.

## REFERENCES

1. Association AP. Diagnostic and statistical manual of mental disorders (5th ed.) Washington D.C., 2013.
2. Green B. Post-traumatic stress disorder: symptom profiles in men and women. Curr Med Res Opin. 2003;19:200–4.
3. Frans O, Rimmo PA, Aberg L, Fredrikson M. Trauma exposure and post-traumatic stress disorder in the general population. Acta Psychiatr Scand. 2005;111:291–9.
4. Kessler RC, Berglund P, Demler O, Jin R, Merikangas KR, Walters EE. Lifetime prevalence and age-of-onset distributions of DSM-IV disorders in the national comorbidity survey replication. Arch Gen Psychiatry. 2005;62:593–602.
5. Richter-Levin G, Stork O, Schmidt MV. Animal models of PTSD: a challenge to be met. Mol Psychiatry. 2019;24:1135–56.
6. Besnard A, Sahay A. Adult hippocampal neurogenesis, fear generalization, and stress. Neuropsychopharmacology. 2016;41:24–44.
7. Liberzon I, Abelson JL. Context processing and the neurobiology of post-traumatic stress disorder. Neuron. 2016;92:14–30.
8. Kheirbek MA, Klemenhagen KC, Sahay A, Hen R. Neurogenesis and generalization: a new approach to stratify and treat anxiety disorders. Nat Neurosci. 2012;15:1613–20.
9. Colgin LL, Moser EI, Moser MB. Understanding memory through hippocampal remapping. Trends Neurosci. 2008;31:469–77.
10. Gilbert PE, Kesner RP, Lee I. Dissociating hippocampal subregions: double dissociation between dentate gyrus and CA1. Hippocampus. 2001;11:626–36.
11. Leutgeb JK, Leutgeb S, Moser MB, Moser EI. Pattern separation in the dentate gyrus and CA3 of the hippocampus. Science. 2007;315:961–6.
12. McClelland JL, Goddard NH. Considerations arising from a complementary learning systems perspective on hippocampus and neocortex. Hippocampus. 1996;6:654–65.
13. McHugh TJ, Jones MW, Quinn JJ, Balthasar N, Coppari R, Elmquist JK, et al. Dentate gyrus NMDA receptors mediate rapid pattern separation in the hippocampal network. Science. 2007;317:94–99.
14. Treves A, Rolls ET. Computational constraints suggest the need for two distinct input systems to the hippocampal CA3 network. Hippocampus. 1992;2:189–99.
15. Fenton AA. Neuroscience. Where am I? Science. 2007;315:947–9.
16. Stefanelli T, Bertollini C, Luscher C, Muller D, Mendez P. Hippocampal somatostatin interneurons control the size of neuronal memory ensembles. Neuron. 2016;89:1074–85.
17. Fanselow MS, Dong HW. Are the dorsal and ventral hippocampus functionally distinct structures? Neuron. 2010;65:7–19.
18. Kheirbek MA, Drew LJ, Burghardt NS, Costantini DO, Tannenholz L, Ahmari SE, et al. Differential control of learning and anxiety along the dorsoventral axis of the dentate gyrus. Neuron. 2013;77:955–68.
19. Pothuizen HH, Zhang WN, Jongen-Relo AL, Feldon J, Yee BK. Dissociation of function between the dorsal and the ventral hippocampus in spatial learning abilities of the rat: a within-subject, within-task comparison of reference and working spatial memory. Eur J Neurosci. 2004;19:705–12.
20. Yeates DCM, Ussling A, Lee ACH, Ito R. Double dissociation of learned approach-avoidance conflict processing and spatial pattern separation along the dorsoventral axis of the dentate gyrus. Hippocampus 2019;30:596–609.
21. Ritov G, Boltyansky B, Richter-Levin G. A novel approach to PTSD modeling in rats reveals alternating patterns of limbic activity in different types of stress reaction. Mol Psychiatry. 2016;21:630–41.
22. Seo DO, Carillo MA, Chih-Hsiung Lim S, Tanaka KF, Drew MR. Adult hippocampal neurogenesis modulates fear learning through associative and nonassociative mechanisms. J Neurosci. 2015;35:11330–45.
23. Weeden CS, Roberts JM, Kamm AM, Kesner RP. The role of the ventral dentate gyrus in anxiety-based behaviors. Neurobiol Learn Mem. 2015;118:143–9.
24. Fu J, Xing X, Han M, Xu N, Piao C, Zhang Y, et al. Region-specific roles of the prelimbic cortex, the dorsal CA1, the ventral DG and ventral CA1 of the hippocampus in the fear return evoked by a sub-conditioning procedure in rats. Neurobiol Learn Mem. 2016;128:80–91.
25. Banasr M, Soumier A, Hery M, Mocaer E, Daszuta A. Agomelatine, a new antidepressant, induces regional changes in hippocampal neurogenesis. Biol Psychiatry. 2006;59:1087–96.
26. Samuels BA, Anacker C, Hu A, Levinstein MR, Pickenhagen A, Tsetsenis T, et al. 5-HT1A receptors on mature dentate gyrus granule cells are critical for the antidepressant response. Nat Neurosci. 2015;18:1606–16.
27. Wu MV, Hen R. Functional dissociation of adult-born neurons along the dorsoventral axis of the dentate gyrus. Hippocampus. 2014;24:751–61.
28. Sodic L, Anticevic V, Britvic D, Ivkosic N. Short-term memory in Croatian war veterans with posttraumatic stress disorder. Croat Med J. 2007;48:140–5.
29. Hayes JP, Hayes S, Miller DR, Lafleche G, Logue MW, Verfaellie M. Automated measurement of hippocampal subfields in PTSD: Evidence for smaller dentate gyrus volume. J Psychiatr Res. 2017;95:247–52.
30. Wang Z, Neylan TC, Mueller SG, Lenoci M, Truran D, Marmar CR, et al. Magnetic resonance imaging of hippocampal subfields in posttraumatic stress disorder. Arch Gen Psychiatry. 2010;67:296–303.
31. Adamec R, Hebert M, Blundell J, Mervis RF. Dendritic morphology of amygdala and hippocampal neurons in more and less predator stress responsive rats and more and less spontaneously anxious handled controls. Behav Brain Res. 2012;226:133–46.
32. Cohen H, Kozlovsky N, Matar MA, Zohar J, Kaplan Z. Distinctive hippocampal and amygdalar cytoarchitectural changes underlie specific patterns of behavioral disruption following stress exposure in an animal model of PTSD. Eur Neuropsychopharmacol. 2014;24:1925–44.
33. Yang C, Shirayama Y, Zhang JC, Ren Q, Hashimoto K. Regional differences in brain-derived neurotrophic factor levels and dendritic spine density confer resilience to inescapable stress. Int J Neuropsychopharmacol 2015;18:pyu121.
34. Zohar J, Yahalom H, Kozlovsky N, Cwikel-Hamzany S, Matar MA, Kaplan Z, et al. High dose hydrocortisone immediately after trauma may alter the trajectory of PTSD: interplay between clinical and animal studies. Eur Neuropsychopharmacol. 2011;21:796–809.
35. Herrmann L, Ionescu IA, Henes K, Golub Y, Wang NX, Buell DR, et al. Long-lasting hippocampal synaptic protein loss in a mouse model of posttraumatic stress disorder. PLoS One. 2012;7:e42603.
36. Guenthner CJ, Miyamichi K, Yang HH, Heller HC, Luo L. Permanent genetic access to transiently active neurons via TRAP: targeted recombination in active populations. Neuron. 2013;78:773–84.
37. Bangasser DA, Wicks B. Sex-specific mechanisms for responding to stress. J Neurosci Res. 2017;95:75–82.
38. Oyola MG, Handa RJ. Hypothalamic-pituitary-adrenal and hypothalamic-pituitary-gonadal axes: sex differences in regulation of stress responsivity. Stress. 2017;20:476–94.
39. Henckens M, Printz Y, Shamgar U, Dine J, Lebow M, Drori Y, et al. CRF receptor type 2 neurons in the posterior bed nucleus of the stria terminalis critically contribute to stress recovery. Mol Psychiatry. 2017;22:1691–1700.
40. Lebow M, Neufeld-Cohen A, Kuperman Y, Tsoory M, Gil S, Chen A. Susceptibility to PTSD-like behavior is mediated by corticotropin-releasing factor receptor type 2 levels in the bed nucleus of the stria terminalis. J Neurosci. 2012;32:6906–16.
41. Grandjean J, Schroeter A, Batata I, Rudin M. Optimization of anesthesia protocol for resting-state fMRI in mice based on differential effects of anesthetics on functional connectivity patterns. Neuroimage. 2014;1022:838–47.
42. Thiel G, Synapsin I. synapsin II, and synaptophysin: marker proteins of synaptic vesicles. Brain Pathol. 1993;3:87–95.
43. Kennedy MB. The postsynaptic density at glutamatergic synapses. Trends Neurosci. 1997;20:264–8.
44. Shiraishi-Yamaguchi Y, Furuichi T. The Homer family proteins. Genome Biol. 2007;8:206.
45. Kerloch T, Clavreul S, Goron A, Abrous DN, Pacary E. Dentate granule neurons generated during perinatal life display distinct morphological features compared with later-born neurons in the mouse hippocampus. Cereb Cortex. 2019;29:3527–39.
46. Marrocco J, Mairesse J, Ngomba RT, Silletti V, Van Camp G, Bouwalerh H, et al. Anxiety-like behavior of prenatally stressed rats is associated with a selective reduction of glutamate release in the ventral hippocampus. J Neurosci. 2012;32:17143–54.
47. Goodman L, Baddeley D, Ambroziak W, Waites CL, Garner CC, Soeller C, et al. N-terminal SAP97 isoforms differentially regulate synaptic structure and

postsynaptic surface pools of AMPA receptors. Hippocampus. 2017;27:668–82.
48. Meyer D, Bonhoeffer T, Scheuss V. Balance and stability of synaptic structures during synaptic plasticity. Neuron. 2014;82:430–43.
49. Baczyk M, Alami NO, Delestree N, Martinot C, Tang L, Commisso B, et al. Synaptic restoration by cAMP/PKA drives activity-dependent neuroprotection to motoneurons in ALS. J Exp Med 2020;217.
50. Denny CA, Kheirbek MA, Alba EL, Tanaka KF, Brachman RA, Laughman KB, et al. Hippocampal memory traces are differentially modulated by experience, time, and adult neurogenesis. Neuron. 2014;83:189–201.
51. Root CM, Denny CA, Hen R, Axel R. The participation of cortical amygdala in innate, odour-driven behaviour. Nature. 2014;515:269–73.
52. DeNardo LA, Liu CD, Allen WE, Adams EL, Friedmann D, Fu L, et al. Temporal evolution of cortical ensembles promoting remote memory retrieval. Nat Neurosci. 2019;22:460–9.
53. Kitamura T, Ogawa SK, Roy DS, Okuyama T, Morrissey MD, Smith LM, et al. Engrams and circuits crucial for systems consolidation of a memory. Science. 2017;356:73–78.
54. Zoellner LA, Pruitt LD, Farach FJ, Jun JJ. Understanding heterogeneity in PTSD: fear, dysphoria, and distress. Depress Anxiety. 2014;31:97–106.
55. Yehuda R. Status of glucocorticoid alterations in post-traumatic stress disorder. Ann N Y Acad Sci. 2009;1179:56–69.
56. Klaassens ER, Giltay EJ, Cuijpers P, van Veen T, Zitman FG. Adulthood trauma and HPA-axis functioning in healthy subjects and PTSD patients: a meta-analysis. Psychoneuroendocrinology. 2012;37:317–31.
57. Morris MC, Compas BE, Garber J. Relations among posttraumatic stress disorder, comorbid major depression, and HPA function: a systematic review and meta-analysis. Clin Psychol Rev. 2012;32:301–15.
58. Mehta D, Binder EB. Gene × environment vulnerability factors for PTSD: the HPA-axis. Neuropharmacology. 2012;62:654–62.
59. Zaba M, Kirmeier T, Ionescu IA, Wollweber B, Buell DR, Gall-Kleebach DJ, et al. Identification and characterization of HPA-axis reactivity endophenotypes in a cohort of female PTSD patients. Psychoneuroendocrinology. 2015;55:102–15.
60. Geerse GJ, van Gurp LC, Wiegant VM, Stam R. Individual reactivity to the open-field predicts the expression of cardiovascular and behavioural sensitisation to novel stress. Behav Brain Res. 2006;175:9–17.
61. Nalloor R, Bunting K, Vazdarjanova A. Predicting impaired extinction of traumatic memory and elevated startle. PLoS One. 2011;6:e19760.
62. Christiansen DM, Elklit A. Risk factors predict post-traumatic stress disorder differently in men and women. Ann Gen Psychiatry. 2008;7:24.
63. Jaksic N, Brajkovic L, Ivezic E, Topic R, Jakovljevic M. The role of personality traits in posttraumatic stress disorder (PTSD). Psychiatr Danub. 2012;24:256–66.
64. Brunet A, Sanche S, Manetti A, Aouizerate B, Ribereau-Gayon R, Charpentier S, et al. Peritraumatic distress but not dissociation predicts posttraumatic stress disorder in the elderly. Int Psychogeriatr. 2013;25:1007–12.
65. Mellman TA, David D, Bustamante V, Fins AI, Esposito K. Predictors of post-traumatic stress disorder following severe injury. Depress Anxiety. 2001;14:226–31.
66. Laposa JM, Rector NA. The prediction of intrusions following an analogue traumatic event: peritraumatic cognitive processes and anxiety-focused rumination versus rumination in response to intrusions. J Behav Ther Exp Psychiatry. 2012;43:877–83.
67. Kaouane N, Porte Y, Vallee M, Brayda-Bruno L, Mons N, Calandreau L, et al. Glucocorticoids can induce PTSD-like memory impairments in mice. Science. 2012;335:1510–3.
68. Qu Y, Yang C, Ren Q, Ma M, Dong C, Hashimoto K. Regional differences in dendritic spine density confer resilience to chronic social defeat stress. Acta Neuropsychiatr. 2018;30:117–22.
69. Klugmann M, Symes CW, Leichtlein CB, Klaussner BK, Dunning J, Fong D, et al. AAV-mediated hippocampal expression of short and long Homer 1 proteins differentially affect cognition and seizure activity in adult rats. Mol Cell Neurosci. 2005;28:347–60.
70. Anacker C, Luna VM, Stevens GS, Millette A, Shores R, Jimenez JC, et al. Hippocampal neurogenesis confers stress resilience by inhibiting the ventral dentate gyrus. Nature. 2018;559:98–102.
71. Bernier BE, Lacagnina AF, Ayoub A, Shue F, Zemelman BV, Krasne FB, et al. Dentate gyrus contributes to retrieval as well as encoding: evidence from context fear conditioning, recall, and extinction. J Neurosci. 2017;37:6359–71.
72. Madronal N, Delgado-Garcia JM, Fernandez-Guizan A, Chatterjee J, Kohn M, Mattucci C, et al. Rapid erasure of hippocampal memory following inhibition of dentate gyrus granule cells. Nat Commun. 2016;7:10923.
73. Drew LJ, Kheirbek MA, Luna VM, Denny CA, Cloidt MA, Wu MV, et al. Activation of local inhibitory circuits in the dentate gyrus by adult-born neurons. Hippocampus. 2016;26:763–78.
74. Tallent MK. Somatostatin in the dentate gyrus. Prog Brain Res. 2007;163:265–84.
75. Lesuis SL, Brosens N, Immerzeel N, van der Loo RJ, Mitric M, Bielefeld P, et al. Glucocorticoids promote fear generalization by increasing the size of a dentate gyrus engram cell population. Biol Psychiatry. 2021;90:494–504.
76. Liu X, Ramirez S, Pang PT, Puryear CB, Govindarajan A, Deisseroth K, et al. Optogenetic stimulation of a hippocampal engram activates fear memory recall. Nature. 2012;484:381–5.
77. Roy DS, Kitamura T, Okuyama T, Ogawa SK, Sun C, Obata Y, et al. Distinct neural circuits for the formation and retrieval of episodic memories. Cell. 2017;170:1000–12 e1019.
78. Frankland PW, Bontempi B. The organization of recent and remote memories. Nat Rev Neurosci. 2005;6:119–30.
79. Winocur G, Moscovitch M. Memory transformation and systems consolidation. J Int Neuropsychol Soc. 2011;17:766–80.
80. Hainmueller T, Bartos M. Parallel emergence of stable and dynamic memory engrams in the hippocampus. Nature. 2018;558:292–6.
81. Khalaf O, Resch S, Dixsaut L, Gorden V, Glauser L, Graff J. Reactivation of recall-induced neurons contributes to remote fear memory attenuation. Science. 2018;360:1239–42.
82. Lacagnina AF, Brockway ET, Crovetti CR, Shue F, McCarty MJ, Sattler KP, et al. Distinct hippocampal engrams control extinction and relapse of fear memory. Nat Neurosci. 2019;22:753–61.
83. Admon R, Milad MR, Hendler T. A causal model of post-traumatic stress disorder: disentangling predisposed from acquired neural abnormalities. Trends Cogn Sci. 2013;17:337–47.
84. Pitman RK, Rasmusson AM, Koenen KC, Shin LM, Orr SP, Gilbertson MW, et al. Biological studies of post-traumatic stress disorder. Nat Rev Neurosci. 2012;13:769–87.
85. Fiala JC, Spacek J, Harris KM. Dendritic spine pathology: cause or consequence of neurological disorders? Brain Res Brain Res Rev. 2002;39:29–54.
86. Nakashiba T, Cushman JD, Pelkey KA, Renaudineau S, Buhl DL, McHugh TJ, et al. Young dentate granule cells mediate pattern separation, whereas old granule cells facilitate pattern completion. Cell. 2012;149:188–201.
87. Sahay A, Wilson DA, Hen R. Pattern separation: a common function for new neurons in hippocampus and olfactory bulb. Neuron. 2011;70:582–8.
88. Cameron HA, McKay RD. Adult neurogenesis produces a large pool of new granule cells in the dentate gyrus. J Comp Neurol. 2001;435:406–17.
89. Kempermann G, Kuhn HG, Gage FH. Genetic influence on neurogenesis in the dentate gyrus of adult mice. Proc Natl Acad Sci USA. 1997;94:10409–14.
90. Ninkovic J, Mori T, Gotz M. Distinct modes of neuron addition in adult mouse neurogenesis. J Neurosci. 2007;27:10906–11.
91. Tanaka KZ, Pevzner A, Hamidi AB, Nakazawa Y, Graham J, Wiltgen BJ. Cortical representations are reinstated by the hippocampus during memory retrieval. Neuron. 2014;84:347–54.
92. Tayler KK, Tanaka KZ, Reijmers LG, Wiltgen BJ. Reactivation of neural ensembles during the retrieval of recent and remote memory. Curr Biol. 2013;23:99–106.

## ACKNOWLEDGEMENTS

MJAGH was supported by Veni Grant 863.15.008 and J.R.H. by Vidi Grant 864.10.003 awarded by the Netherlands Organization for Scientific Research.

## AUTHOR CONTRIBUTIONS

Concept and design: JRH, TK, MJAGH. Data acquisition and analysis: BCJD, DvdG, CT, MvB, LM, LvA, MJAGH. Statistical analysis: BCJD, DvdG, CT, MvB, LM, LvA, MJAGH. Drafting of the manuscript: MJAGH. Financial support: JRH, TK, MJAGH. Manuscript revision: BCJD, JRH, TK, MJAGH.

## COMPETING INTERESTS

The authors declare no competing interests.

## ADDITIONAL INFORMATION

**Supplementary information** The online version contains supplementary material available at https://doi.org/10.1038/s41398-022-02264-7.

**Correspondence** and requests for materials should be addressed to Tamas Kozicz or Marloes J.A.G. Henckens.